



Simultaneous voltammetric detection of 5-hydroxyindole-3-acetic acid and 5-hydroxytryptamine using a glassy carbon electrode modified with conducting polymer and platinised carbon nanofibers

Zina Fredj^{1,2} · MounirBen Ali^{1,2} · Baljit Singh³ · Eithne Dempsey⁴

Received: 30 April 2018 / Accepted: 3 August 2018 / Published online: 13 August 2018
© Springer-Verlag GmbH Austria, part of Springer Nature 2018

Abstract

The authors describe a method for simultaneous voltammetric determination of 5-hydroxytryptamine (serotonin; 5-HT) and its metabolite 5-hydroxyindoleacetic acid (5-HIAA). A glassy carbon electrode was modified with poly(pyrrole-3-carboxylic acid) and with platinised carbon nanofibers to obtain a sensor that can quantify 5-HT and 5-HIAA with detection limits of 10 nM and 20 nM, respectively. The peak currents, best measured at voltages of 170 mV and 500 mV (vs. Ag/AgCl) for 5-HT and 5-HIAA, increase linearly in the 0.01–100 μ M concentration range for both analytes. The method was successfully applied to the quantitation of 5-HT and 5-HIAA in spiked artificial urine samples, and the sensor can be used up to 10 days.

Keywords 5-Hydroxyindole-3-acetic acid · 5-Hydroxytryptamine · Pt nanocomposites · Pyrrole-3-carboxylic acid · Stripping square wave voltammetry · Quantitation in artificial urine

Introduction

5-Hydroxytryptamine (5-HT) or serotonin is a neurotransmitter, which plays a crucial physiological role with respect to cardiovascular function, muscle contraction, endocrine regulation and depression [1, 2] and is implicated in migraine and schizophrenia [3]. Disorders like bipolar disease and anxiety

have been associated with decreasing levels of 5-HT [4–7]. 5-Hydroxyindole-3-acetic acid (5-HIAA) is a product of 5-HT breakdown and is excreted in the urine, having a regulatory action on the homeostatic state [8]. Moreover, certain tumor cells have been found to produce excess 5-HT and 5-HIAA and altered urinary levels may act as an early diagnostic marker [9–11]. Overall, reliable and accurate quantitation of 5-HT and 5-HIAA levels in biological samples is clinically significant, particularly in challenging biological matrices [12]. Spectrophotometry and chromatographic approaches have been used in the determination of 5-HT and 5-HIAA including fluorescence [13], chemiluminescence (CL) [14] and LC-MS/MS [15]. A recent spectrophotometric approach by Guillermo Bracamonte et al. enabled dual detection of both serotonin and 5-HIAA in urine [16].

The pioneering work by Adams [17] and Wightman [18] and the resulting fast response times and low detection limits allowed development of electroanalytical approaches which complement conventional chromatographic/spectroscopic methods [19–23]. In this context, Gomez *et al.* reported a sensor based on single-walled carbon nanotubes (SWCNT), multi-walled carbon nanotubes (MWCNT) and graphene for 5-HT and melatonin detection [24]. Recently, Sharma *et al.* compiled a review article regarding chemically modified electrodes for serotonin detection [25] and Makrlíková *et al.* have

Electronic supplementary material The online version of this article (<https://doi.org/10.1007/s00604-018-2949-5>) contains supplementary material, which is available to authorized users.

✉ Eithne Dempsey
Eithne.dempsey@mu.ie

¹ Higher Institute of Applied Sciences and Technology of Sousse, GREENS-ISSAT, University of Sousse, 4003 IbnKhaldoun, Sousse, Tunisia

² NANOMISENE Lab, LR16CRMN01, Centre for Research on Microelectronics and Nanotechnology of Sousse, Technopole of Sousse, Sahloul, 4034 Sousse, Tunisia

³ MiCRA Biodiagnostics, Centre of Applied Science for Health, Institute of Technology Tallaght, Tallaght, D24 FKT9, Dublin 24, Ireland

⁴ Department of Chemistry, Maynooth University, Maynooth, Co. Kildare, Ireland

reported the voltammetric detection of 5-HIAA at screen-printed electrodes as one of a number of tumor biomarkers [26]. There are very few electrochemical reports of 5-HIAA detection and to the best of our knowledge, only one prior report of the selective electrochemical dual detection of both 5-HT and 5-HIAA [8] based on Au modified ITOs.

In this work, we report fabrication of a sensitive and selective electrochemical sensor for the rapid simultaneous determination of 5-HT and 5-HIAA at conducting polymer (pyrrole-3-carboxylic acid) nanostructured surfaces. The approach takes advantage of high surface to volume ratio for platinised carbon nanofibers (prepared *in-house*). Pyrrole based conducting polymers adhere well to Pt surfaces and hence to the nanocomposites employed [27]. Electrochemical interrogation of 5-HT and 5-HIAA was achieved via cyclic voltammetry (CV) and stripping square wave voltammetry (SSWV). The experimental results showed that the modified electrode displayed a significant and selective response to dual detection of 5-HT and 5-HIAA. The co-existence of dopamine (DOP), ascorbic acid (AA) and uric acid (UA) at physiological levels showed minimal interference with respect to the determination of 5-HT and 5-HIAA, which was also possible in simulated human urine samples.

Experimental

Materials

Serotonin, creatinine sulfate monohydrate, 5-Hydroxyindole-3-acetic acid, uric acid (99%), dopamine hydrochloride (98%), L-Ascorbic acid 99%, pyrrole-3-carboxylic acid ($\geq 96\%$), lithium perchlorate (99.99%), sodium carbonate (anhydrous, 99.5%), were purchased from Sigma–Aldrich, Dublin (<https://www.sigmaaldrich.com/ireland.html>). Aqueous solutions were prepared with ultra-pure water (Sartorius, Germany). The nanomaterials used were synthesised *in house* (platinised carbon nanofibers - 20% w/w Pt loading). The stock solutions of serotonin were prepared daily by dissolution in an appropriate amount of 0.1 M HCl followed by storage at +4 °C. Phosphate buffer were prepared from 0.1 M $\text{KH}_2\text{PO}_4/\text{K}_2\text{HPO}_4$ solutions (99%, Fluka (<https://www.lab-honeywell.com/products/brands/fluka/>)). Artificial urine samples were prepared according to the recipe provided by Brooks and Keevil [28]. The solution was comprised of 1.1 mM lactic acid, 2.0 mM citric acid, 25 mM sodium bicarbonate, 170 mM urea, 2.5 mM calcium chloride, 90 mM sodium chloride, 2.0 mM magnesium sulfate, 10 mM sodium sulfate, 7.0 mM potassium dihydrogen phosphate, 7.0 mM dipotassium hydrogen phosphate, and 25 mM ammonium chloride all in Millipore water. The pH of the solution was adjusted to 6.0 via the addition of 1.0 M hydrochloric acid.

The Pt-decorated carbon nanofibers material ($\text{Pt}_{19.2}/\text{f-CNF}_{80.8}$) used in this work was synthesised in-house and reported previously [29, 30]. Carbon nanofibers (PR-19-XT-LHT) were supplied by Pyrograf Products Inc. (<https://www.ptonline.com/suppliers/pyrogra>) and were milled (processed by 1-pass (AM-1)) by the company according to requirements. These “open” nanofibers were then functionalised prior to Pt nanoparticle decoration. The precursor hexachloroplatinic acid ($\text{H}_2\text{PtCl}_6 \cdot 6\text{H}_2\text{O}$), sulfuric acid (H_2SO_4), nitric acid (HNO_3), ethylene glycol, potassium hydroxide and Nafion® (5% solution in a mixture of lower aliphatic alcohols and water) were purchased from Sigma Aldrich.

Apparatus

Stripping mode square wave voltammetry was performed using an electrochemical workstation - CH Instruments Inc. 920 in phosphate buffer (pH 7.4), with a conventional three-electrode cell (5 mL) at room temperature. A modified glassy carbon electrode (3 mm diameter) served as the working electrode, while platinum wire and a standard Ag/AgCl electrode (filled with 3 M KCl) were employed as the counter and reference electrodes, respectively. Prior to electrochemical measurements, the glassy carbon electrode was polished with 1.0, 0.3, and 0.05 μm alumina powders, sonicated in acetone and distilled water and dried at room temperature.

The surface morphology and distribution for $\text{Pt}_{19.2}/\text{f-CNF}_{80.8}$ was characterised using transmission electron microscopy (TEM) with a JEOL 2011 operated at 200 kV using a LaB₆ filament equipped with a Gatan Multiscan Camera 794 and dark field scanning TEM (DF-STEM) with a JEOL 2100F operated at 200 kV using a field emission electron source equipped with a Gatan Ultrascan Camera [29, 30]. For TEM measurements, samples were suspended in isopropyl alcohol, sonicated and drop cast onto Cu grids and dried overnight at 30 °C. The elemental analysis employed EDS and the surface morphology of the synthesised material were also examined using JSM SEM (JEOL 6390 LV) over a range of magnifications and accelerating voltages [30]. The detailed information on SEM/TEM, EDS/EDX, TGA/DTG, XRD, XPS and electrochemical characterisation are described in our reported work [29, 30].

Procedures

f-CNF Carbon nanofibers (CNF) were functionalised for efficient Pt dispersion and decoration. Milled nanofibers were treated with sonication for 2 h in concentrated $\text{H}_2\text{SO}_4/\text{HNO}_3$ acid solution (3: 1, 125 mL acid solution diluted to 250 mL with distilled water) and kept overnight followed by filtration and washing with distilled water in order to remove the residual catalyst and carbon impurities. The sonication was

repeated but in the concentrated acid mixture for 30 min. Followed by dilution of the acid mixture (3 times, v/v) with distilled water and again sonicated (1.5 h). The solution was kept overnight, diluted, filtered and washed with sufficient distilled water to reach neutral pH and then dried under vacuum at 90 °C for 13 h. The functionalised carbon nanofibers were labeled f-CNF.

Pt_{19,2}/f-CNF_{80,8} The functionalisation and Pt nanoparticle decoration procedures were described in detail in our previous work [29, 30] and outlined briefly in ESM. Pt_{19,2}/f-CNF_{80,8} is labeled as Pt/f-CNF hereafter.

Electrode preparation

Glassy carbon electrode electrodes were polished with 1.0, 0.3, and 0.05 µm alumina powders, on polishing pads and sonicated in acetone and ethanol, washed with deionised water and dried using Argon at room temperature. The electrode was then dipped in 1 M H₃PO₄ to remove any adhered matter, followed by washing several times with double distilled water. A typical suspension of the synthesised material was prepared by suspending the Pt/f-CNF in a water-isopropyl alcohol mixture (3:1). The calculated amount of Nafion® solution (1%) was added to the suspension followed by sonication (20 min) for uniform dispersion [29, 30].

Electrochemical polymerisation of polypyrrole-3-carboxylic acid on Pt/f-CNF/GCE electrode

The electrochemical polymerisation of monomer pyrrole-3-carboxylic acid (P3CA) was performed using potential cycling (20 cycles) between 0.0 V and +1.25 V at a scan rate of 20 mV s⁻¹ in an aqueous solution containing 20.0 mM P3CA in 0.1 M LiClO₄ and 0.1 M Na₂CO₃ at the Pt/f-CNF modified glassy carbon electrode. This resulted in an irreversible wave at 0.45 V vs. Ag/AgCl (ESM Fig. S1). The so formed p(P3CA)/Pt/f-CNF/GCE electrode was then washed with deionised water and stored at room temperature.

Electrochemical procedure for quantitation via stripping square wave voltammetry

Following electrode surface modification, pulse voltammetric analysis was exploited for analytical signaling and discrimination. This involved an accumulation step at 0.4 V for 120 s in unstirred solution followed by an anodic scan from -0.2 - 0.8 V with superimposed square wave at 20 Hz, pulse amplitude 5 mV. Background buffer studies were performed in advance to ensure no contribution from the electrolyte. Peak currents were background subtracted and used as analytical signal for calibration data ($n = 3$).

Results and discussion

Rationale for functionalised nanocomposite material selection and surface characterisation [Pt_{19,2}/f-CNF_{80,8}]

Carbon supported nanomaterials as electrode modifiers have advantages of electrocatalytic activity and fast electron transfer kinetics with reduced graphene-oxide-cobalt oxide nanoparticles in serotonin sensing being the subject of a recent report [31]. Prior work in our group established chemical synthetic approaches for the efficient dispersion and inside/outside decoration of 2.5 nm Pt nanoparticles on open ended, activated carbon nanofibers. In order to further improve the neurotransmitter signal transduction and provide selectivity, pyrrole-3-carboxylic acid was electrochemically polymerised onto the Pt_{19,2}/f-CNF_{80,8} glassy carbon electrode and exhibited good adhesion and performance. To our knowledge this is the first such use of platinised nanocomposites which provide high surface area supports for polymeric deposition, targeting dual quantitation of 5-HT and 5-HIAA in buffered solutions and artificial urine samples.

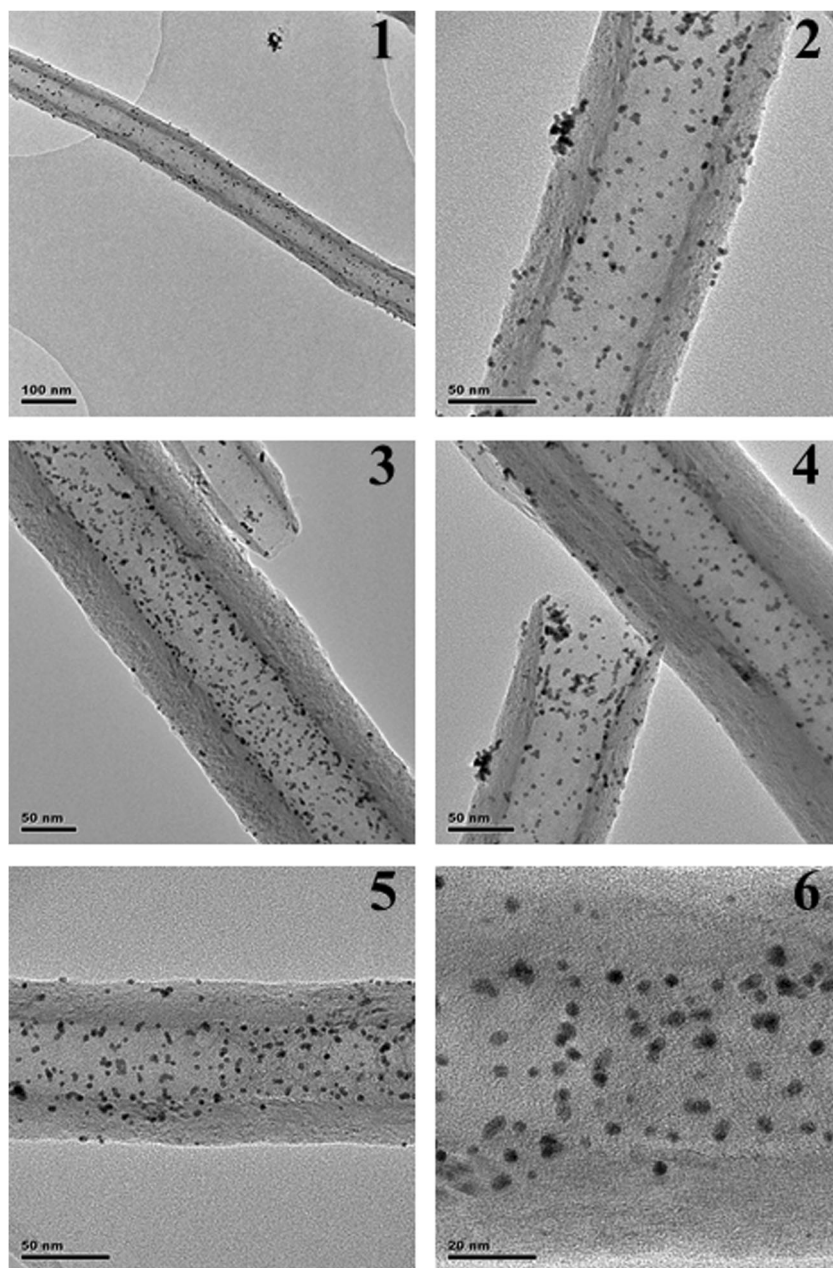
TEM studies provided clear information on the dispersion, decoration, and size of the Pt nanoparticles on carbon nanofibers and were well dispersed and embedded within the walls and the outer surface of the carbon nanofibers. The open ends of the nanofibers were clearly confirmed by TEM analysis as can be seen from images 3 & 4 (Fig. 1) and the nanofibers exhibited a large central hollow core and opened ends, which together realised a significant portion of exposed and reactive edges, providing excellent Pt nanoparticle dispersion and decoration.

Particle size distribution analysis from randomly chosen areas confirmed that the average particle size was 2.4 nm. The Pt nanoparticles were crystalline in a face-centered cubic (fcc) structure, space group Fm3m and cell parameter 3.92 °Å [29]; dark field scanning TEM (DF-STEM), PSD, EDS/EDX, SEM, TGA, XRD, XPS studies and electrochemical interrogation confirmed the identity and presence of Pt in decorated nanofibers [29, 30].

Overall, the nanoparticle distribution and decoration of carbon nanofibers was achieved as a result of the following:

- i. The synthetic procedure (aging time, solvent system and polarity characteristics) makes for the diffusion of the precursor Pt salt solution both inside and outside of the nanofibers. Capillary action can possibly help to transport the precursor salt solution into the inner side morphology of the carbon nanofibers, which is further improved by the aging time given to precursor salt solution and carbon nanofibers. The pH was maintained at 10.5 (by KOH addition) during the synthesis, which further improved the dispersion/decoration of nanoparticles, attributed to the electrostatic stabilisation of nanoparticles by the adsorbed hydroxyl ions.

Fig. 1 Transmission electron micrographs (1) scale bar 100 nm (2)–(5) scale bar 50 and (6) scale bar 20 nm, showing excellent Pt nanoparticle decoration and distribution on carbon nanofibers for Pt_{19.2}/f-CNF_{80.8}. TEM images confirmed the open ends of carbon nanofibers (image 3&4). The thermogravimetric (TGA/DTG) analysis confirmed the Pt loading (19.2%) onto the nanofibers in agreement with a synthetic procedure and accordingly the material was labeled as Pt_{19.2}/f-CNF_{80.8} [29]



- ii. Opened ends of nanofibers, active inner wall morphology and the activated outer wall via acid functionalisation, make it possible to achieve effective nanoparticle dispersion and optimum utilisation of both nanofibers and precious Pt content. The chemical functionalisation leads to the formation of groups such as C–O–C/C–OH/C=O/COO etc. on the surfaces of nanofibers (confirmed by XPS analysis) [29, 30], which are known to act as anchoring sites for nanoparticles.

The above-described features of Pt/f-CNF make these materials capable of improved stability due to a strong metallic nanoparticle- nanofiber support interaction, avoiding metal

dissolution during e.g. sensor applications. The Pt/f-CNF was then deployed in catalytic/electrochemical neurochemical detection, taking advantage of the low fixed metallic (Pt) loading and enhancement of the available support surface area for in this case electrodeposition of the P3CA electropolymerised film.

Firstly, 5-HT was examined by cyclic voltammetry at a Pt/f-CNF modified glassy carbon electrode at pH 7.2 resulting in an anodic peak at 0.42 V vs. Ag/AgCl. Fig. S2 ESM shows the cyclic voltammograms which also compares the relative signals arising from bare (GCE) and modified (Pt/f-CNF/GCE) electrodes. The oxidation current signal was linear over the range 0.5–100 μ M. However, the Pt/f-CNF modified GCE electrode did not enable voltammetric signal separation of a

mixture of both 5-HT and 5-HIAA, hence the requirement for the subsequent deposition of the P3CA electropolymer in order to enable discrimination of the target analytes.

Square wave stripping voltammetric determination of 5-hydroxytryptamine at p(P3CA)/Pt/f-CNF modified glassy carbon electrode

Firstly, the dependence of stripping peak current (i_p) on accumulation potential (E_{acc}) was evaluated over the range 0.2 to 1.0 V for 10 μM serotonin in phosphate buffer (pH 7.2) at the polymer modified Pt/f-CNF GCE surface. The results obtained showed that the peak current values for anodic square wave voltammetry (-0.2 to 0.8 V) are optimal with the use of an accumulation potential of 0.4 V vs. Ag/AgCl (see Fig. 2a). The effects of accumulation time on the voltammetric response of 5-HT (10 μM), prior to anodic stripping, were examined over a range of accumulation times, (Fig. 2b) at constant $E_{acc} = 0.4$ V. This was followed by square wave voltammetry (SSWV) from -0.2 to 0.8 V (step potential = 5 mV, frequency = 20 Hz, pulse amplitude 5 mV), resulting in an analytical signal due to the oxidation ($E_p = 0.42$ V) of the serotonin molecule at the p(P3CA)/Pt/f-CNF/GCE electrode surface. A gradual increase in oxidation peak response was

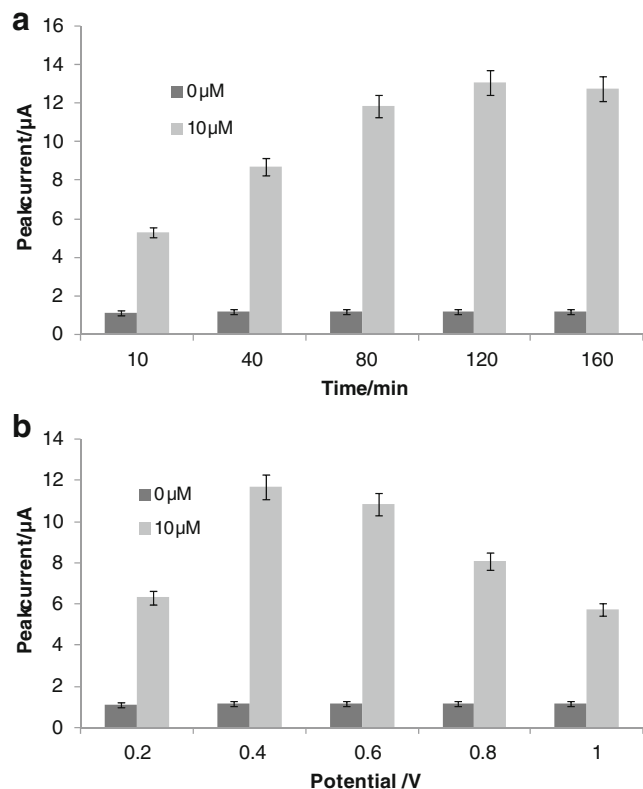


Fig. 2 a The blank and SSWV responses for 10 μM 5-HT achieved under different accumulation potentials (0.2 – 1.0 V); b Influence of accumulation time (10 – 160 min) on blank and 10 μM 5-HT signal at p(P3CA)/Pt/f-CNF/GCE in 0.1 M phosphate buffer

observed with increasing time up to 120 s, after which a steady signal for 5-HT was achieved. Therefore, 120 s was chosen as the optimal value and employed in the case of subsequent experiments.

Under optimal experimental conditions, the electrochemical oxidation of 5-HT was performed at 0.4 V vs Ag/AgCl for 120 s in non-stirred solution, followed by anodic stripping square wave voltammetry (Fig. 3a) at a Pt/f-CNF/GCE (in the first instance). A well-defined response at $+0.52$ V vs. Ag/AgCl was evident, corresponding to the oxidation of serotonin over the range 0.025 – 100 μM . Coefficient of determination (R^2) was 0.965 , limit of detection (LOD) 10 nM (defined as $3\sigma/\text{slope}$; $n = 3$), linear relation eq. $Y = 8.88 (\pm 0.27) X + 5.78 (\pm 0.195)$. Signal reproducibility was investigated by measuring the response of the 5-HT analyte at

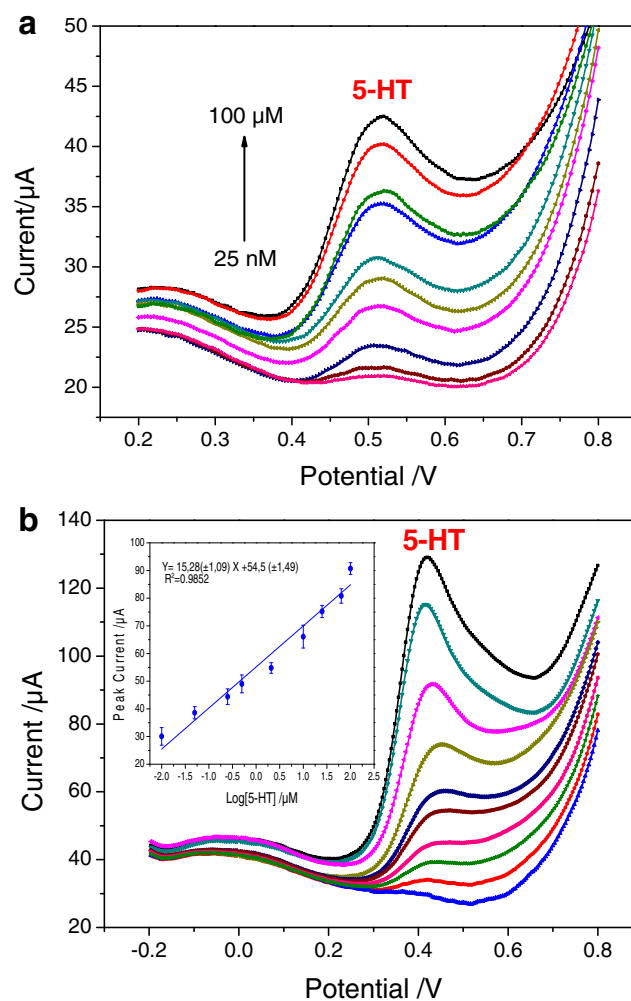


Fig. 3 a Blank and anodic SSWV of 5-HT over the range 25 nM– 100 μM at Pt/f-CNF modified GCE. b Blank and anodic SSWV curves of 5-HT concentration over the range 10 nM– 100 μM at p(P3CA)/Pt/f-CNF/GCE from -0.2 to 0.8 V, (insert) calibration plot for SSWV data showing peak current (i_p) vs. 5-HT conc. over the range 10 nM– 100 μM ($n = 3$) in phosphate buffer, Accumulation time 120 s. at $E_{acc} = 0.4$ V, frequency 20 Hz, pulse amplitude 5 mV

100 nM and 10 μM with $n=6$ replicates. The coefficients of variation for both measured concentrations were 3.8 and 4.6%, respectively at the Pt/f-CNF modified glassy carbon electrode.

Secondly, the p(P3CA)/Pt/f-CNF/GCE electrode underwent SSWV under similar operating conditions resulting in peak currents which increased over the range 10 nM - 100 μM (Fig. 3b) with a 3 fold increase in signal relative to data in Fig. 3a in the absence of polymer. A well-defined response at the lower potential of +0.42 V vs. Ag/AgCl was evident, corresponding to the quantitative oxidation of serotonin over this range.

The corresponding calibration curve is presented in Fig. 3b and resulted in a linear relationship equation of $Y = 15.28 (\pm 1.09) X + 54.5 (\pm 1.49)$ with a linear regression constant ($R^2 = 0.9852$ for $n = 3$) observed over the concentration range 10 nM–100 μM . The detection limit value was determined as 0.1 nM ($S/N = 3$).

Determination of 5-hydroxyindole-3-acetic acid via stripping square wave voltammetry

SSWV curves for 5-HIAA over a range of concentrations were recorded under the experimental conditions above. It is observed that the peak current increased with increasing 5-HIAA concentration (Fig. 4), and a linear relationship over the range 10 nM to 100 μM with a regression equation of $Y = 22.8 (\pm 1.46) X + 44.88 (\pm 1.75)$ was obtained, with LOD of 1 nM (see insert for 5-HIAA calibration curve).

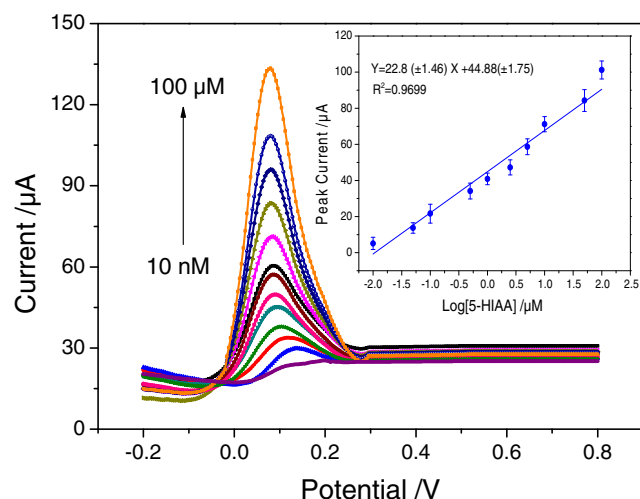


Fig. 4 SSWV of 5-HIAA over range 10 nM–100 μM in phosphate buffer at p(P3CA)/Pt/f-CNF/GCE. Accumulation time 120 s. at $E_{acc} = 0.4$ V, step potential 5 mV, frequency 20 Hz, pulse amplitude 5 mV. (Insert) Calibration plot for SSWV data - peak current (i_p vs. 5-HIAA conc. over the range 10 nM–100 μM)

Simultaneous determination of 5-hydroxyindole-3-acetic acid and 5-hydroxytryptamine

Simultaneous quantitation of both 5-hydroxyindole-3-acetic acid (5-HIAA) and 5-hydroxytryptamine (5-HT) at the p(P3CA)/Pt/f-CNF/GCE electrode followed and the stripping square wave curve recorded following application of a positive potential of 0.4 V for 120 s. Two well-defined anodic peaks at $\sim +0.17$ V and 0.5 V vs. Ag/AgCl were observed with good separation achieved (Fig. 5a). Corresponding calibration curves are shown in Fig. 5b.

The analytes were detected over the dynamic range 10 nM to 100 μM . The regression equation for the simultaneous detection of 5-HT and 5-HIAA based sensor was $Y1 = 17.02X + 27.78$, where X is the logarithm of 5-HT concentration (μM); Y is the SSWV peak current (μA) with a coefficient of determination (R^2) of 0.9834, and the limit of detection (LOD) was calculated to be 10 nM (defined as $3\sigma/\text{slope}$; $n = 3$) $Y2 =$

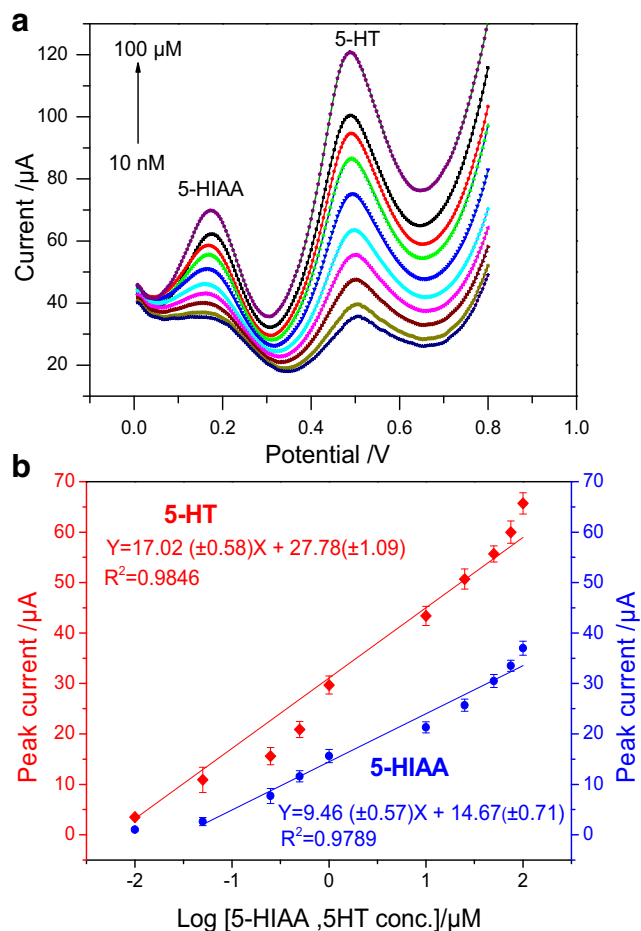


Fig. 5 a Simultaneous SSWV determination of 5-HT and 5-HIAA at p(P3CA)/Pt/f-CNF/GCE in phosphate buffer of pH 7.2. **b** Calibration plot of peak current (i_p vs. 5-HIAA and 5-HT conc. over the range 10 nM–100 μM) at p(P3CA)/Pt/f-CNF/GCE in phosphate buffer of pH 7.2

Table 1 Influence of selected interferents (1000 fold excess) on peak currents of 5-HT (50 nM) and 5-HIAA (50 nM) at p(P3CA)/Pt/f-CNF/GCE

Interfering ions	5-HIAA detected (μA)	5-HT detected (μA)
No interferent	8 ± 0.68	11 ± 0.83
Uric acid (50 μM)	7.6 ± 0.55	10.5 ± 0.41
Ascorbic acid (50 μM)	6.4 ± 0.24	9.6 ± 0.72
Dopamine (50 μM)	7.1 ± 0.14	9.3 ± 0.36

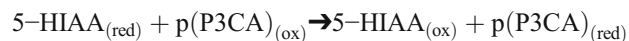
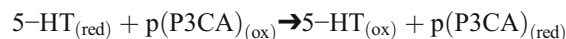
$9.038X + 14.6778$, where X is the logarithm of 5-HIAA concentration (μM); Y is the SSVV peak current (μA), with a coefficient of determination (R^2) of 0.9384, and the limit of detection (LOD) was calculated to be 20 nM (defined as $3\sigma/\text{slope}$; $n = 3$).

The peak current of 5-HT in the dual system at p(P3CA)/Pt/f-CNF/GCE was enhanced relative to that of 5-HIAA at Pt/f-CNF/GCE as indicated by the slope of the individual and mixed calibration plots. There was also an anodic shift (100 mV) in the peak positions in each case indicating an alteration in properties of the adsorbed layer relative to individual analyte accumulation at 0.4 V vs. Ag/AgCl. This could possibly be due to chemical interactions upon adsorption making oxidation relatively more difficult. At the pH employed, and based on the $\text{p}K_a$ values of the analytes we expect that 5-HIAA be negatively charged (carboxylate group) and that 5-HT is positive (due to protonated amine group). As a result, a competitive electrostatic surface effect may occur during deposition where -vely charged 5-HIAA may be repelled by the charged p(P3CA) layer while +vely charged 5-HT may be attracted to the surface and hence more readily available for stripping and quantitation.

The influence of pH on the sensor response was examined for 50 nM 5-HT and 5-HIAA over the range 3.0–11.0 (see Fig. S3 ESM) and data indicated no significant change in signal. Hence the response appeared insensitive with respect to pH. The role of scan rate on the response to 50 nM 5-HT at the modified electrode was also examined (see Fig. S4 ESM) resulting in a diffusion controlled linear relationship between peak current and square root scan rate.

Redox behaviour arises as a result of the $1e^- 1H^+$ oxidation of the alcoholic moiety of the aromatic system in the case of both 5-HT and 5-HIAA. This process is accelerated in the

presence of both the platinised nanocomposite and the doped conducting polymer, resulting in a 3-fold increase in sensitivity for both 5-HT and 5-HIAA respectively and a cathodic shift in oxidation potential.



The catalytic effect may include a dopant interaction with the oxidised p(P3CA) film e.g. 5-HIAA may act as charge compensator to balance the doped conducting polymer, while 5-HT, being positive could electrostatically interact with the carboxylate group on the p(P3CA) film. The modifiers also realise surface selectivity with respect to structurally related catecholamines such as dopamine.

The repeatability of the electrode was evaluated by detecting 0.1 μM of the 5HT and 5-HIAA in buffer, and the peak current of five successive assays gave a relative standard deviation (RSD) of 2.5%. The stability of the electrode was investigated by measuring its response to 0.1 μM levels of each neurotransmitter. When not in use, the electrode was stored at 4 °C in a refrigerator. After a week, the current response of the electrode retained up to 89.5% of its initial value. Inter-electrode precision was examined with five individual electrodes fabricated independently by the same process, resulting in RSD of 6% for the 0.1 μM 5HT and 5-HIAA signal. These studies indicated that the electrode surface had good regeneration properties upon reuse, maintaining film integrity and stability.

Interference studies

The effect of some common electroactive interferences on the simultaneous voltammetric response of 5HT and 5-HIAA was examined by performing square wave voltammetry measurements in the absence and presence of interfering substances. Relevant electroactive interferents selected included ascorbic acid (AA), uric acid (UA) and dopamine (DOP). Stripping square wave voltammetric measurements were performed in buffer (pH 7.2) containing a mixture of 50 μM AA ($E_p = 0.16$ V), 50 μM UA ($E_p = 0.28$ V) and 50 μM DOP ($E_p = 0.41$ V vs. Ag/AgCl). The same experiment was then repeated in the presence of 50 nM 5-HT and 50 nM 5-HIAA (see Fig.

Table 2 The actual and measured concentration of 5-HIAA and 5-HT in the artificial urine sample ($n = 3$)

Actual concentration	5-HIAA measured concentration ($n = 3$)	5-HT measured concentration ($n = 3$)
50 nM	(48 ± 6.85) nM	(56 ± 6.35) nM
500 nM	(557 ± 34.2) nM	(477 ± 64.2) nM
1.0 μM	(1.6 ± 0.07) μM	(1.2 ± 0.23) μM
10 μM	(8.95 ± 0.27) μM	(9.05 ± 6.7) μM

Table 3 Analytical parameters obtained in previous studies regarding electrochemical detection of 5-HT and 5-HIAA

References	Transducer/catalyst	Technique used	Sensitivity and analytical performance
Gomez FJV et al. [24]	Carbon nanotubes and graphene modified carbon screen-printed electrodes (CSPEs)	Differential pulse voltammetry	MT (melatonin) Detection limit: 1.1 and 5-HT Detection limit 0.4 μM
Gu Ran et al. [23]	Multiwalled carbon nanotubes, chitosan and poly(p-aminobenzenesulfonic) modified glassy carbon electrode	Differential pulse voltammetry	5-HT Linear range: 0.10.1 mM Detection limit: 80 nM.
Goyal et al. [8]	SWCNT/GCE Au nanoparticle/ITO	Osteryoung square wave voltammetry	5-HT Linear range:0.1–100 μM & Detection limit: 5 nM 5-HIAA Linear range:0.1–100 μM & Detection limit: 7 nM
Anna Makrlíková and al. [33]	Screen printed electrodes	Differential Pulse voltammetry	5-HIAA Linear range: 0.2–100 μM & Limit of quantitation 0.4 μM
M. Satyanarayana and al. [34]	Multiwalled carbon nanotube – chitosan composite modified glassy carbon electrode	Cyclic voltammetry and electrochemical impedance spectroscopy	5-HT Linear range: 5×10^{-8} – 1.6×10^{-5} M & Detection limit: 50 μM
A.C. Anithaa and al. [35]	Gamma ray irradiated tungsten trioxide nanoparticles modified glassy carbon electrodes	Cyclic voltammetry and differential pulse voltammetry	5-HT Linear range: 0.01–600 μM & Detection limit: 1.42 nM
Yuting, Wang [36]	MWNT/ZnO/chitosan composites modified screen-printed electrode	Cyclic voltammetry and square wave voltammetry	5-HT Linear range:0.05–1 μM & Detection limit: 10 nM
This work	Polypyrrole 3- carboxylic acid @ platinised carbon nanofibers	Stripping square wave voltammetry	5-HT Linear range: 0.01–100 μM & Detection limit: 10 nM 5-HIAA Linear range: 0.01–100 μM & Detection limit: 20 nM <i>Individual LOD 0.1 and 1 nM for 5-HT and 5-HIAA resp.</i>

S5 ESM and data Table 1). It was found that there was negligible effect on the peak current intensity of 5-HT in the presence of 1000 fold DOP, UA and AA concentration. The Pt nanocomposite was dispersed in a Nafion/IPA solution and this perfluorosulphonated polymer will repel such anionic species while also realising discrimination with respect to co-existing neurotransmitters. As indicated in Table 1 the modified transducer enables the discrimination of the electrochemical oxidation signals of these four substances. Moreover, the electrochemical oxidation peak of serotonin and 5-hydroxyindole-3- acetic acid was separated from interfering species indicating that the p(P3CA)/Pt/f-CNF/GCE exhibited high selectivity toward 5-HT and 5-HIAA. It has been reported that the oxidation of dopamine at carbon nanotube modified carbon fiber microelectrode occurred at a potential close to 5-HIAA and 5-HT [32], however, using our approach dopamine does not interfere up to 1000-fold excess.

Quantification in artificial urine samples:

As the 5-HT/5-HIAA urinary ratio is an important marker for various diseases and age-related physiological conditions, it was considered necessary to detect these biomolecules in this sample type. Artificial urine solutions were prepared according to the literature for recovery studies of 5-HT and 5-HIAA. Samples were then spiked with different quantities of 5-HT and 5-HIAA (0.05 μM , 0.5 μM , 1 μM and 10 μM) and % recovery established. Data is presented in Table 2 and indicates a good correlation between the measured and actual concentration of 5-HIAA and the 5HT in the artificial urine samples with the sensor capable of quantitation in this matrix. The average % recovery across this concentration range was 96.48%.

A comparison of the p(P3CA)/Pt/f-CNF/GCE with other reported modified electrodes for 5-HIAA detection is given in Table 3 and results in comparable analytical performance, with the key feature being accomplishment of dual voltammetric detection of these important analytes in simulated urine samples with good selectivity, peak separation and reusability.

Conclusions

Simultaneous voltammetric detection of 5-hydroxyindole-3-acetic acid and 5-hydroxytryptamine at an electropolymerised glassy carbon transducer modified with platinised carbon nanofibers was successfully achieved. Successful polymerisation of the pyrrole-3 carboxylic acid monomer onto immobilised platinised carbon nanofibers realised a stable surface architecture realising repeatable simultaneous and sensitive voltammetry of 5-HT and 5-HIAA. Optimisation of anodic stripping square wave voltammetric conditions resulted in detection limits of 10 nM and 20 nM for dual detection of 5-

HT and 5-HIAA respectively. The linear range was 0.01–100 μM in both cases and well separated anodic peaks (+0.17 V and 0.5 V vs. Ag/AgCl for 5-HT and 5-HIAA respectively) were observed under physiological conditions and in the presence of electroactive interferents. Recovery studies from spiked simulated urine demonstrated average values of 104.5% (5-HT) and 114.3% (5-HIAA) and sensor lifetime was >10 days. The time to result was <2.5 min which is in line with on-site rapid testing requirements. Overall, this work advances simultaneous electrochemical detection of 5-HT and its metabolite 5-HIAA, both of which are significant clinical targets as neurotransmitter and tumour biomarkers.

Acknowledgements This work was partially funded by the “SMARTCANCERSENS” project Marie Curie IRSES staff exchange programme - Grant Agreement PIRSES-GA 2012-318053.

Compliance with ethical standards The author(s) declare that they have no competing interests.

References

- Houghton LA, Atkinson W, Whitaker RP et al (2003) Increased platelet depleted plasma 5-hydroxytryptamine concentration following meal ingestion in symptomatic female subjects with diarrhoea predominant irritable bowel syndrome. *Gut* 52:663–670
- Some M, Helander A (2002) Urinary excretion patterns of 5-hydroxyindole-3-acetic acid and 5-hydroxytryptophol in various animal species: implications for studies on serotonin metabolism and turnover rate. *Life Sci* 71:2341–2349
- Garver DL, Davis JM (1979) Biogenic amine hypotheses of affective disorders. *Life Sci* 24:383–394
- Wang Z, Liang Q, Wang Y, Luo G (2003) Carbon nanotube-intercalated graphite electrodes for simultaneous determination of dopamine and serotonin in the presence of ascorbic acid. *J Electroanal Chem* 540:129–134. [https://doi.org/10.1016/S0022-0728\(02\)01300-1](https://doi.org/10.1016/S0022-0728(02)01300-1)
- Zen JM, Chen IL, Shih Y (1998) Voltammetric determination of serotonin in human blood using a chemically modified electrode. *Anal Chim Acta* 369:103–108
- Chatzitofis A, Nordström P, Hellström C, Arver S, Åsberg M, Jokinen J (2013) CSF 5-HIAA, cortisol and DHEAS levels in suicide attempters. *Eur Neuropsychopharmacol J Eur Coll Neuropsychopharmacol* 23:1280–1287. <https://doi.org/10.1016/j.euroneuro.2013.02.002>
- Moberg T, Nordström P, Forslund K, Kristiansson M, Åsberg M, Jokinen J (2011) CSF 5-HIAA and exposure to and expression of interpersonal violence in suicide attempters. *J Affect Disord* 132:173–178. <https://doi.org/10.1016/j.jad.2011.01.018>
- Goyal RN, Oyama M, Gupta VK, Singh SP, Sharma RA (2008) Sensors for 5-hydroxytryptamine and 5-hydroxyindole acetic acid based on nanomaterial modified electrodes. *Sens Actuators B Chem* 134:816–821. <https://doi.org/10.1016/j.snb.2008.06.027>
- Torney WP, FitzGerald RJ (1995) The clinical and laboratory correlates of an increased urinary 5-hydroxyindoleacetic acid. *Postgrad Med J* 71:542–545
- Banik S, Lahiri T (2000) Increase in brain serotonin level and concomitant reduction in food intake and body weight of mice bearing chemically - induced Fibrosarcoma. *Biomed Res* 21:255–261. <https://doi.org/10.2220/biomedres.21.255>
- Dursun SM, Whitaker RP, Andrews H, Reveley MA (1999) Effects of natural ageing on plasma 5-HT turnover in humans. *Hum Psychopharmacol Clin Exp* 12:365–367. [https://doi.org/10.1002/\(SICI\)1099-1077\(199707/08\)12:4<365::AID-HUP879>3.0.CO;2-2](https://doi.org/10.1002/(SICI)1099-1077(199707/08)12:4<365::AID-HUP879>3.0.CO;2-2)
- Xu H, Zhang W, Wang D, Zhu W, Jin L (2007) Simultaneous determination of 5-hydroxyindoleacetic acid and 5-hydroxytryptamine in urine samples from patients with acute appendicitis by liquid chromatography using poly(bromophenol blue) film modified electrode. *J Chromatogr B Analyt Technol Biomed Life Sci* 846:14–19. <https://doi.org/10.1016/j.jchromb.2006.08.021>
- Nohta H, Yukizawa T, Ohkura Y, Yoshimura M, Ishida J, Yamaguchi M (1997) Aromatic glycinonitriles and methylamines as pre-column fluorescence derivatization reagents for catecholamines. *Anal Chim Acta* 344:233–240. [https://doi.org/10.1016/S0003-2670\(96\)00614-9](https://doi.org/10.1016/S0003-2670(96)00614-9)
- Zhang L, Zhao Y, Huang J, Zhao S (2014) Simultaneous quantification of 5-hydroxyindoleacetic acid and 5-hydroxytryptamine by capillary electrophoresis with quantum dot and horseradish peroxidase enhanced chemiluminescence detection. *J Chromatogr B Analyt Technol Biomed Life Sci* 967:190–194. <https://doi.org/10.1016/j.jchromb.2014.07.002>
- Moriarty M, Lee A, O’Connell B, Kelleher A, Keeley H, Furey A (2011) Development of an LC-MS/MS method for the analysis of serotonin and related compounds in urine and the identification of a potential biomarker for attention deficit hyperactivity/hyperkinetic disorder. *Anal Bioanal Chem* 401:2481–2493. <https://doi.org/10.1007/s00216-011-5322-7>
- Bracamonte AG, Veglia AV (2011) Spectrofluorimetric determination of serotonin and 5-hydroxyindoleacetic acid in urine with different cyclodextrin media. *Talanta* 83:1006–1013. <https://doi.org/10.1016/j.talanta.2010.11.013>
- Adams RN (1976) Probing brain chemistry with electroanalytical techniques. *Anal Chem* 48:1126A–1138A. <https://doi.org/10.1021/ac50008a001>
- Leszczyszyn DJ, Jankowski JA, Viveros OH et al (1990) Nicotinic receptor-mediated catecholamine secretion from individual chromaffin cells. Chemical evidence for exocytosis *J Biol Chem* 265:14736–14737
- Mozaffari SA, Chang T, Park S-M (2010) Self-assembled monolayer as a pre-concentrating receptor for selective serotonin sensing. *Biosens Bioelectron* 26:74–79. <https://doi.org/10.1016/j.bios.2010.05.015>
- Liu M, Crussière M, Hèlard JF (2010) Enhanced two-dimensional data-aided channel estimation for TDS-OFDM. In: 2010 4th international conference on signal processing and communication systems. Pp 1–7
- Wang F, Wu Y, Lu K, Ye B (2013) A simple but highly sensitive and selective calixarene-based voltammetric sensor for serotonin. *Electrochim Acta* 87:756–762. <https://doi.org/10.1016/j.electacta.2012.09.033>
- Zhao H, Bian X, Galligan JJ, Swain GM (2010) Electrochemical measurements of serotonin (5-HT) release from the Guinea pig mucosa using continuous amperometry with a boron-doped diamond microelectrode. *Diam Relat Mater* 19:182–185
- Ran G, Chen C, Gu C (2015) Serotonin sensor based on a glassy carbon electrode modified with multiwalled carbon nanotubes, chitosan and poly(p-aminobenzenesulfonate). *Microchim Acta* 182:1323–1328. <https://doi.org/10.1007/s00604-015-1454-3>
- Gomez FJV, Martín A, Silva MF, Escarpa A (2015) Screen-printed electrodes modified with carbon nanotubes or graphene for simultaneous determination of melatonin and serotonin. *Microchim Acta* 182:1925–1931. <https://doi.org/10.1007/s00604-015-1520-x>
- Sharma S, Singh N, Tomar V, Chandra R (2018) A review on electrochemical detection of serotonin based on surface modified

- electrodes. *Biosens Bioelectron* 107:76–93. <https://doi.org/10.1016/j.bios.2018.02.013>
26. Makrlíková A, Ktena E, Economou A, Fischer J, Navrátil T, Barek J, Vyskočil V (2016) Voltammetric determination of tumor biomarkers for Neuroblastoma (Homovanillic acid, Vanillylmandelic acid, and 5-Hydroxyindole-3-acetic acid) at screen-printed carbon electrodes. *Electroanalysis* 29:146–153. <https://doi.org/10.1002/elan.201600534>
 27. Ravichandran R, Sundarajan S, Venugopal JR, Mukherjee S, Ramakrishna S (2010) Applications of conducting polymers and their issues in biomedical engineering. *J R Soc Interface* 7:S559–S579. <https://doi.org/10.1098/rsif.2010.0120.focus>
 28. Brooks T, Keevil CW (1997) A simple artificial urine for the growth of urinary pathogens. *Lett Appl Microbiol* 24:203–206
 29. Singh B, Dempsey E, Dickinson C, Laffir F (2012) Inside/outside Pt nanoparticles decoration of functionalised carbon nanofibers (Pt19.2/f-CNF80.8) for sensitive non-enzymatic electrochemical glucose detection. *Analyst* 137:1639–1648. <https://doi.org/10.1039/C2AN16146J>
 30. Singh B, Dempsey E (2013) Exceptional Pt nanoparticle decoration of functionalised carbon nanofibers: a strategy to improve the utility of Pt and support material for direct methanol fuel cell applications. *RSC Adv* 3:2279–2287. <https://doi.org/10.1039/C2RA21862C>
 31. Dinesh B, Veeramani V, Chen S-M, Saraswathi R (2017) In situ electrochemical synthesis of reduced graphene oxide-cobalt oxide nanocomposite modified electrode for selective sensing of depression biomarker in the presence of ascorbic acid and dopamine. *J Electroanal Chem* 786:169–176. <https://doi.org/10.1016/j.jelechem.2017.01.022>
 32. Swamy BEK, Venton BJ (2007) Carbon nanotube-modified microelectrodes for simultaneous detection of dopamine and serotonin in vivo. *Analyst* 132:876–884. <https://doi.org/10.1039/b705552h>
 33. Antuña-Jiménez D, Blanco-López MC, Miranda-Ordieres AJ, Lobo-Castañón MJ (2015) Artificial enzyme-based catalytic sensor for the electrochemical detection of 5-hydroxyindole-3-acetic acid tumor marker in urine. *Sens Actuators B Chem* 220:688–694. <https://doi.org/10.1016/j.snb.2015.05.109>
 34. Satyanarayana M, Koteswara Reddy K, Vengatajalabathy Gobi K (2014) Nanobiocomposite Based Electrochemical Sensor for Sensitive Determination of Serotonin in Presence of Dopamine, Ascorbic Acid and Uric Acid In Vitro. *Electroanalysis* 26:2365–2372. <https://doi.org/10.1002/elan.201400243>
 35. Anithaa AC, Asokan K, Sekar C (2017) Highly sensitive and selective serotonin sensor based on gamma ray irradiated tungsten trioxide nanoparticles. <https://doi.org/10.1016/j.snb.2016.07.098>
 36. Wang Y, Wang S, Tao L, Min Q, Xiang J, Wang Q, Xie J, Yue Y, Wu S, Li X, Ding H (2015) A disposable electrochemical sensor for simultaneous determination of norepinephrine and serotonin in rat cerebrospinal fluid based on MWNTs-ZnO/chitosan composites modified screen-printed electrode. *Biosens Bioelectron* 65:31–38. <https://doi.org/10.1016/j.bios.2014.09.099>